

pubs.acs.org/NanoLett Letter

Frequency Stabilization and Optically Tunable Lasing in Colloidal **Quantum Dot Superparticles**

Steven J. Neuhaus, Emanuele Marino, Christopher B. Murray, and Cherie R. Kagan*



Cite This: Nano Lett. 2023, 23, 645-651



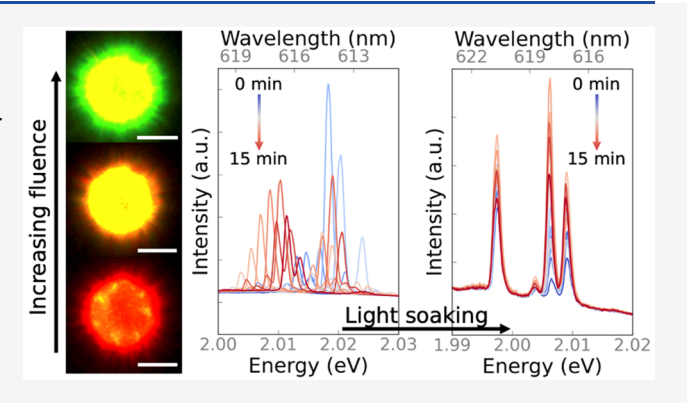
ACCESS I

III Metrics & More

Article Recommendations

Supporting Information

ABSTRACT: Self-assembled superparticles composed of colloidal quantum dots establish microsphere cavities that support optically pumped lasing from whispering gallery modes. Here, we report on the time- and excitation fluence-dependent lasing properties of CdSe/CdS quantum dot superparticles. Spectra collected under constant photoexcitation reveal that the lasing modes are not temporally stable but instead blue-shift by more than 30 meV over 15 min. To counter this effect, we establish a high-fluence lightsoaking protocol that reduces this blue-shift by more than an order of magnitude to 1.7 ± 0.5 meV, with champion superparticles displaying mode blue-shifts of <0.5 meV. Increasing the pump fluence allows for optically controlled, reversible, color-tunable redto-green lasing. Combining these two paradigms suggests that quantum dot superparticles could serve in applications as low-cost, robust, solution-processable, tunable microlasers.



KEYWORDS: nanocrystal, quantum dot, superparticle, supraparticle, lasing, optical stability, tunable laser

olloidal semiconductor nanocrystals, or quantum dots (QDs), have generated tremendous interest due, in part, to their remarkable optical properties: their absorption and photoluminescence (PL) spectra are size-tunable, and modern synthetic techniques enable near-unity quantum yields.² Moreover, QDs and their assemblies are entirely solutionprocessable,3 affording a high degree of flexibility toward optoelectronic device integration.^{4,5}

In particular, colloidal QDs are a highly studied medium for optical gain because their energetically well-separated, discrete electronic states theoretically promote low lasing thresholds, high-temperature stability, and large gain coefficients.^{6–8} Since the first demonstrations of optical gain in QDs, 9,10 researchers have focused intensely on pragmatic designs for QD lasers, which have historically been impeded by fast, nonradiative Auger recombination in population-inverted QDs. There have been substantial efforts to reduce the effects of Auger recombination by synthesizing both thick-shelled core/shell QDs¹¹⁻¹³ (sometimes termed "giant nanocrystals") and compositionally graded QDs. 14-16

Drawing on the successes of synthetic methods which allow for nanocrystals with a broad range of tailorable physical properties, there is a growing interest in using nanocrystals as building blocks for mesoscale assemblies known as superparticles or supraparticles (SPs). 17-19 These SPs allow for functionalities otherwise unobserved from their constituent nanocrystals alone. For example, combining red-, green-, and blue-emitting QDs into a single SP enables white-light generation from the SP as a whole, ²⁰ and the formation of micrometer-scale spherical SPs effectively combines the constituent nanocrystals (e.g., QDs or upconverting nanophosphors) into dielectric microresonators which support whispering gallery modes. 21,22 Coupling these whispering gallery modes to the gain properties of constituent QDs enables SP lasing.^{23,24}

Robust SP lasers could serve as a portable platform for in situ applications (such as biosensing) that are not accessible to conventionally fabricated microresonators, which are typically bound to rigid substrates. The sensitivity of QD SPs to their environment has been demonstrated by the tunability of their emission through chemical composition, 20 chemical triggers, 22 and ultraviolet exposure.²² Previous work on microfabricated QD resonators has shown lasing that can be actively tuned using the pump fluence.²⁵ Extending this paradigm to SPs would allow for a more attractive platform for the development of new applications based on inexpensive, tunable, and robust microlasers.

Here, we report on the time- and fluence-dependent lasing properties of QD-based SPs. We show that the lasing modes of the as-cast SPs are not temporally stable under constant

Received: November 15, 2022 Revised: December 29, 2022 Published: January 5, 2023





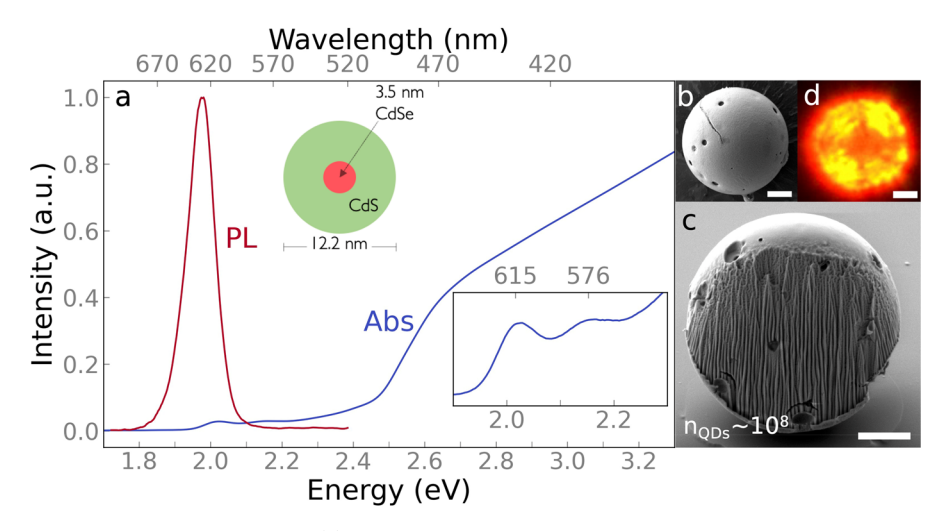


Figure 1. QD properties and superparticle morphology. (a) Optical absorption and PL spectra of dispersions of CdSe/CdS core—shell QD building blocks used in the assembly of QD SPs. The upper inset depicts the QD morphology, and the lower inset highlights the excitonic structure in the absorption spectrum. (b) Top-down and (c) cross-sectional SEM images of QD SPs. (d) Optical dark-field microscopy image of a single QD SP. All scale bars are 2 μ m.

photoexcitation but instead blue-shift by more than 30 meV over 15 min of continuous operation, consistent with a photoinduced change in the refractive index of the QD SPs. We counter this effect by establishing a straightforward, high-fluence light-soaking protocol that dramatically improves the spectral stability of the lasing modes by more than an order of magnitude. We also report optically controlled, color-tunable lasing in QD SP microlasers, whereby the pump fluence reversibly controls the color of SP lasing.

We assemble spherical, micrometer-scale SPs from thickshelled, oleate-capped CdSe/CdS core/shell QDs, consisting of 3.5 nm diameter cores and 4.4 nm thick shells. Details on QD synthesis and further characterization are given elsewhere.²⁴ The QD morphology is depicted in Figure 1a along with the absorption and photoluminescence (PL) spectra of QD dispersions. The excitonic features are visible in the red portion of the absorption spectrum shown in Figure 1a, with the 1S and 1P peaks appearing at 615 nm (2.02 eV) and 576 nm (2.15 eV), respectively. The thick CdS shell introduces a dramatic increase in absorbance to the blue of 500 nm (2.5 eV). The PL peak appears at 626 nm (1.98 eV), and the quantum yield is near unity (102 \pm 5%, 500 nm excitation), which is consistent with the characteristics of similar QDs. PL decays from a drop-cast thin film (Figure S1) are fit to a biexponential function with exciton lifetimes having a 10 ns fast component and a 31 ns slow component, which is consistent with previous reports on similar QDs. 13,26

The QDs are assembled into SPs using a source-sink, emulsion-based microfluidic method previously reported by our group. He Briefly, we generate toluene-in-water droplets containing dispersed QDs and introduce smaller hexadecane droplets downstream. The toluene in the source QD droplets progressively transfers to the sink hexadecane droplets, causing the QD source droplets to shrink and driving the assembly of spherical QD SPs. After removing the swollen sink droplets, the SPs are dropcast and allowed to dry on glass substrates and Si wafers for optical (micro)spectroscopy and electron microscopy studies, respectively.

We use scanning electron microscopy (SEM) to characterize the size and morphology of the QD SPs. Representative SEM images of the exterior and cross section of a SP are shown in Figures 1b and 1c, respectively. The SPs have diameters of 9.0 \pm 0.5 μ m and are composed of densely packed QDs but do contain a small number of surface defects and, to a lesser extent, bulk defects. Assuming a packing factor of 0.64 (random close packing) and accounting for a ligand shell around each QD,²⁷ we estimate that each SP is composed of approximately 10⁸ QDs. Because of the high PL quantum yield of the constituent QDs, the SPs appear as bright red particles in an optical dark-field microscope (Figure 1d). The 4-fold symmetry in the optical dark-field image results from the 4-fold symmetry of the dark-field aperture we use, and therefore it appears with the same orientation for every SP that we observe.²⁸

As we and others have observed, the SPs act as microsphere cavities that support whispering gallery modes, 23,24,29-31 while the constituent QDs serve as gain media within the cavity. When exciting the as-cast SPs with 488 nm light from an ultrafast-pumped optical parametric amplifier (see the Supporting Information for experimental details), we observe lasing emission in the red (2.00-2.04 eV, see Figure 2a), which is typically multimode in character. This spectral region corresponds with the blue side of the QD PL spectrum and overlaps with the first excitonic absorption peak (see Figure S2). We measure the lasing thresholds for these modes to be $1200 \pm 400 \,\mu\text{J/cm}^2$ and note that this value is markedly higher than measured thresholds for SPs made from thin-shelled QDs.²³ The presence of lasing on the blue side of the PL envelope and the large threshold fluences are both consistent with previous reports which show that exciton-exciton interactions in thick-shelled QDs cause gain bands to appear toward the blue end of their PL envelopes and thresholds to increase. 32,33 SPs composed of thick-shelled particles are also reported to lase on the blue side of the PL envelope with high thresholds.²³ We note that while le Feber et al.²⁵ report lowthreshold lasing microresonators made from thick-shelled QDs, they utilize a microfabricated ring-resonator geometry that does not suffer from the same bulk attenuation of the incident pump incurred by the microsphere geometry used in this work.

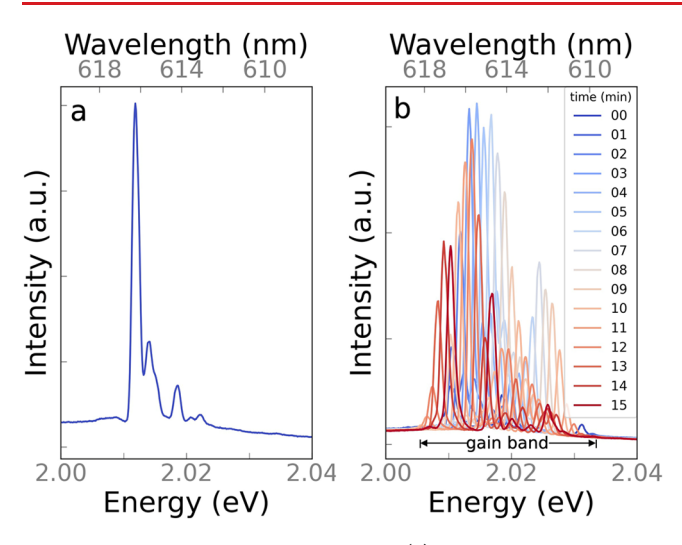


Figure 2. Superparticle lasing spectra. (a) Representative QD SP emission spectrum excited at an excitation fluence of $1.6~\rm mJ/cm^2$ (slightly above the lasing threshold for this SP) and collected using a spectrometer with a 1200 line/mm (0.34 nm/pixel) grating and a CCD camera. (b) Time-dependent emission spectra recorded at an excitation fluence of $1.6~\rm mJ/cm^2$ over 15 min of continuous operation for the same QD SP shown in (a).

We fit the SP lasing modes³⁴ to extract peak positions (E_p) and quality factors ($Q = \frac{E_p}{\Delta E}$, where ΔE is the full width at halfmaximum of the resonance). We find that Q for the as-cast SP lasing modes is 1900 ± 400, with minimum and maximum values of 1100 and 2650, respectively, as shown in Figure S3. Our measured values of Q correspond with cavity lifetimes ($\tau_{\rm c} = \frac{\hbar Q}{E}$, where \hbar is the reduced Planck constant) between $0.36\ \mathrm{and}\ 0.87\ \mathrm{ps}.$ During this time, the gain mode travels a path length $(L_c = \frac{c}{n}\tau_c)$, where c is the speed of light and n is the refractive index of the SP; see SI Note 1) between 24 and 58 μ m, or 2 to 5 times the circumference of the SPs. The distribution in Q that we observe is unsurprising given that modes with different eigenvalues probe different cavity volumes, resulting in different optical losses and therefore different values of Q. Interestingly, these values are comparable with those of similarly sized microfabricated ring resonators made from thick-shell QDs, 25 and exceed those of thin-shell

QD microsphere resonators by factors between 3 and 7.23 We postulate that these differences in Q factors can be attributed to the use of thick-shelled QDs which serve to decrease the number density of QDs in our SPs, thereby reducing optical losses due to reabsorption of emitted photons. Interestingly, when fitting the lasing spectra, modeling each peak as a Gaussian function results in a better fit than when using a Lorentzian function (Figure S4). This discrepancy from theory³¹ along with asymmetry that is often present in the lasing peaks (see Figure S5) suggests that even at the highest spectral resolution obtainable with our spectrometer, what appear to be individual peaks may be composed of multiple unresolved peaks. This is unsurprising given that for a perfect microsphere in a homogeneous medium, modes with the same polarization and polar eigennumber are degenerate in energy,³⁵ which we verify using finite element method simulations (Figure S6). The fact that our real SPs are not perfectly uniform spheres and are placed on a substrate likely breaks some of the symmetries present in the ideal system, thereby slightly lifting the mode degeneracy. If there is unresolved fine structure in the peaks, it would signify that the true values for Q and τ_c are higher than those stated above.

The lasing modes of as-cast SPs are not spectrally stable in time, as shown by emission spectra collected over 15 min (Figure 2b and SI Video 1). Under constant illumination, the whispering gallery modes blue-shift until they reach the highenergy side of the gain band (i.e., the region over which lasing modes can be supported). After this high-energy point, these modes can no longer support lasing. Concurrently, new lasing modes appear at the low-energy side of the gain band and blueshift under constant illumination until they also disappear at the high-energy side of the gain band. We have monitored these spectral shifts for over 3 h and have observed that the peaks continue to shift, albeit within and providing a measure of the ~30 meV gain bandwidth of the QDs in the red. The temporal blue-shift of the lasing modes is consistent with a decrease in the SP refractive index accompanying photoexcited carrier generation. A decrease in refractive index, Δn , of -0.027 is sufficient to shift a lasing mode through the gain band of ~30 meV (see SI Note 1). We attribute this change in refractive index to the charging of the QDs via the capture of carriers by trap states.^{26,36} The spectral instability that we observe may make our as-cast SPs poor candidates for applications such as those that utilize lasing peak position as

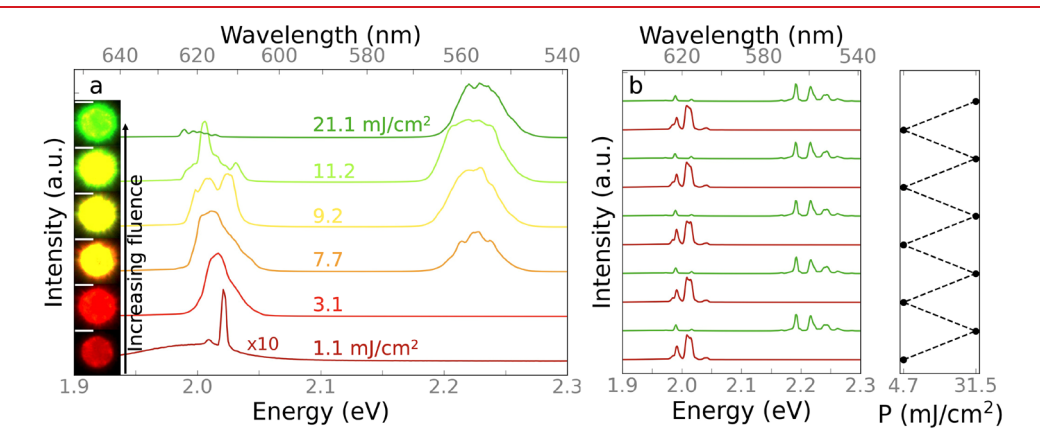


Figure 3. Fluence-dependent lasing properties and reversible tuning. (a) QD SP emission spectra as a function of excitation fluence (ranging from 1.1 to 21.1 mJ/cm²). Insets show corresponding real-space images of the lasing QD SPs. (b) Emission spectra from a different SP as fluences (P) are repeatedly cycled. All scale bars are 5 μ m.

Nano Letters pubs.acs.org/NanoLett Letter

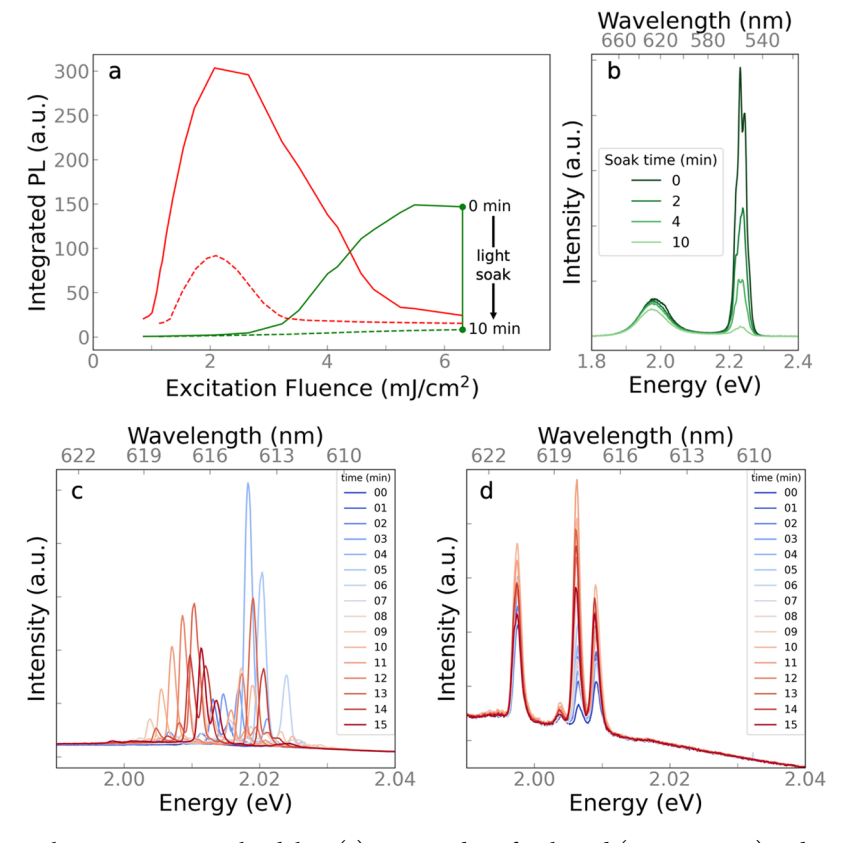


Figure 4. Light-soaking protocol to improve spectral stability. (a) Integrated PL for the red (1.99-2.05 eV) and green (2.17-2.27 eV) spectral components as a function of the excitation fluence as fluence is first increased (solid lines) and then held to light soak the SPs at high fluences of approximately 6 times the lasing threshold. We note that if the fluence remains below this point, then fluence can still be used to reversibly optically tune the red/green lasing. The emission is monitored, and the light soak is concluded when the green emission decreases below that of the red emission at typical times of ~ 10 min. The integrated PL is then collected as the excitation fluence is reduced (dashed lines). (b) Emission spectra recorded over the course of the light-soaking process. Note that the green emission dramatically decreases over time. Time-dependent red SP emission spectra from the same SP (c) before and (d) after light soaking.

an optical environmental sensor.³⁷ Given that the change in refractive index is a property of the constituent QDs, we speculate that peak instability may arise in other optically pumped QD laser architectures.

We also investigate the dependence of the lasing response on excitation fluence. Figure 3a shows that when the excitation intensity is just above threshold, the SPs lase in the red (2.00–2.04 eV), corresponding to emission from the 1S state. As the pump fluence increases, the intensity of red lasing first increases and then decreases as lasing in the green (2.18–2.28 eV) emerges.

At intermediate fluences, PL images of the SPs appear yellow, with shades that vary with the predominance of red and green lasing at lower and higher fluences, respectively. At higher excitation fluences, only green lasing is observed, and the SPs appear green in PL images. This change in lasing color can be reversed by simply lowering the incident fluence, as shown in Figure 3b, where the fluence is repeatedly cycled. We note that collection times for the spectra in Figure 3 are <1 s per spectrum (compared with multiple minutes of light exposure for the data in Figure 2), so we do not observe any noticeable spectral instability in this data. Green emission at higher excitation fluence—both from the 1P state and directly from the bulk-like CdS shell at bluer wavelengths—has been reported from thick-shelled QDs, 13,16 and optical fluencetunable red/green lasing has been reported from microfabricated QD resonators²⁵ but has not been demonstrated in

solution-assembled SPs. The decrease in red lasing as the green lasing increases implies that green lasing from hot carriers occurs faster than carrier cooling, which is consistent with a previous report on tunable red/green lasing (where the green lasing occurs directly from the bulk-like CdS shell).²⁵

We note that the green emission we observe at high fluence (centered around 2.22 eV) is slightly to the blue of the 1P absorption peak (2.15 eV). Exciton-exciton repulsion in thickshelled QDs is expected to blue-shift luminescence at high excitation densities, suggesting that the green emission that we observe may still derive from the 1P state rather than from the bulk-like CdS shell (which has a bandgap of 2.42 eV). To test this hypothesis, we measure fluence-dependent PL from a dropcast film of the constituent QDs and track the evolution of the 1P peak (Figure S7a). We also track the fluence dependence of the green lasing spectral position from a SP (Figure S7b). In both cases, the emission blue-shifts with increasing excitation fluence to being centered at 2.22 eV at high fluence, consistent with the green lasing we observe at high excitation intensities. Thus, we assign the green lasing to emission from the 1P state. We also note that all but the lowest-fluence spectra in Figure 3a appear to show peak broadening; this is, however, simply a result of the loss of resolution associated with recording these spectra using a lowresolution grating (150 lines/mm vs 1200 lines/mm used to record the spectra in Figure 2a,b) in order to show the full spectral range. The broad peaks conceal narrow modes with

Nano Letters pubs.acs.org/NanoLett Letter

high spectral density that cannot be resolved at this lower spectral resolution, as evidenced by Figures 2b and S8.

To address the lasing peak spectral instability, we have developed a light-soaking protocol which stabilizes the red lasing peaks. This light-soaking protocol consists of increasing the excitation fluence until the green emission dominates over the red emission and then further increasing the fluence until we observe the green emission begin to diminish, as depicted in Figure 4a.

The green emission typically begins to decrease at excitation fluences of around 6 times the red lasing threshold. The SP is then exposed to this fluence until the counts of the green peak fall below those of the red peak—typically for exposure times of 10-11 min. Throughout this soak, the green emission decreases permanently and does not return, even after months (Figures 4b and S8). Despite the decrease in the intensity of the green emission observed throughout the light-soaking process, emission spectra still show lasing peaks with high Q factors throughout and after the soak (Figures S3 and S8). This suggests that any decrease in emission intensity can be attributed to alteration of the QDs and not deterioration of the SP microcavity. These observations are consistent with a previous report which showed that light-soaking thick-shelled CdSe/CdS QDs at high fluence irreversibly quenches emission and that this process is driven by activation or creation of surface traps which quickly trap hot carriers before they can cool.³⁶ Additionally, if we are filling trap states, green emission may be impeded by fast Auger recombination involving trapped carriers and the high density of excitons present at the high fluences required for 1P emission.³⁸ Surprisingly, once the incident fluence is lowered following the soak, the SPs still lase in the red, albeit with diminished output power and increased thresholds (Figure 4a, red dashed line). At these lower fluences, however, Auger recombination should be slower, ^{39,40} which may allow for population inversion to again outpace Auger effects, enabling the observed red lasing.

This decrease in lasing intensity is accompanied by a dramatic increase in the spectral stability of the lasing modes (Figure 4c,d). After light-soaking, spectral shifts are reduced by more than an order of magnitude to <2.5 meV (mean: 1.7 \pm 0.5 meV), with champion SPs exhibiting spectral shifts of <0.5 meV. For the four peaks visible in Figure 4d, the average peak shift over 15 min of continuous operation (measured by fitting each spectrum and tracking each peak position) is 0.29 meV, or approximately 0.1 nm, which is negligible compared to the resolution of the spectrometer and the uncertainty of the fitting routine. We posit that the high-fluence, light-soaking process creates and fills a large concentration of trap states in the constituent QDs, and subsequent low-fluence photoexcitation does not measurably change the amount of trapped carriers and thus does not alter the refractive index, giving rise to the resulting spectral stability of lasing. Q factors for the red peaks measured after light soaking (2000 \pm 500) do not vary significantly from those measured before light soaking (1900 \pm 400), as shown in Figure S3. This suggests that the imaginary part of the refractive index and surface scattering from the SPs are both unaffected by light-soaking, as an increase to either would lead to lossier modes and lower Q factors.

In summary, we have shown that light-soaking QD SPs at high-fluence imparts spectral stability to their lasing modes, which are otherwise spectrally unstable under constant illumination. The mechanism driving the as-cast lasing modes to temporally blue-shift is consistent with an

irreversible, photoactivated change in the refractive index of the QD SPs. As such, our light-soaking process may benefit not only QD SP lasers but also other QD-based lasing architectures that may be subject to the same issue. The spectral stability imparted by the light-soaking process increases the viability of the QD SP microlasing architecture for applications. We have also demonstrated multicolor lasing in SPs, which, following traditional paradigms, would require multiple types of QDs to be coassembled. The modality we have demonstrated is not only multicolor, but optically tunable, whereby the incident fluence reversibly controls the lasing color. This feature may allow QD SP lasers to serve as low-cost, robust, solution-processable, multiplexable sources.

ASSOCIATED CONTENT

Supporting Information

The Supporting Information is available free of charge at https://pubs.acs.org/doi/10.1021/acs.nanolett.2c04498.

Additional information about experimental methods and calculation of light-induced change in refractive index and additional figures as referenced in the text (PDF) Spectral evolution of red lasing peaks over 15 min of continuous operation (AVI)

AUTHOR INFORMATION

Corresponding Author

Cherie R. Kagan — Department of Materials Science and Engineering, Department of Chemistry, and Department of Electrical and System Engineering, University of Pennsylvania, Philadelphia, Pennsylvania 19104, United States; ⊚ orcid.org/0000-0001-6540-2009; Email: kagan@seas.upenn.edu

Authors

Steven J. Neuhaus — Department of Materials Science and Engineering, University of Pennsylvania, Philadelphia, Pennsylvania 19104, United States; orcid.org/0000-0002-6754-1165

Emanuele Marino – Department of Chemistry, University of Pennsylvania, Philadelphia, Pennsylvania 19104, United States; Dipartimento di Fisica e Chimica, Università degli Studi di Palermo, 90123 Palermo, Italy

Christopher B. Murray — Department of Materials Science and Engineering and Department of Chemistry, University of Pennsylvania, Philadelphia, Pennsylvania 19104, United States

Complete contact information is available at: https://pubs.acs.org/10.1021/acs.nanolett.2c04498

Author Contributions

E.M. synthesized and characterized the QDs and SPs. S.J.N. devised the light-soaking process, performed lasing measurements, and analyzed data. C.B.M. and C.R.K. supervised the work. S.J.N., E.M., and C.R.K. wrote the manuscript. All authors have given approval to the final version of the manuscript.

Funding

The authors acknowledge the National Science Foundation (NSF) through the University of Pennsylvania Materials Research Science and Engineering Center (MRSEC) under Awards DMR-1720530 for the lasing experiments and DMR-2019444 for the synthesis and characterization of quantum dot

superparticles. C.B.M. acknowledges the Richard Perry University Professorship at the University of Pennsylvania. C.R.K. acknowledges the Stephen J. Angello Professorship at the University of Pennsylvania.

Notes

The authors declare no competing financial interest.

ACKNOWLEDGMENTS

We thank S. M. Thompson for assistance with time-resolved PL measurements.

REFERENCES

- (1) Murray, C. B.; Norris, D. J.; Bawendi, M. G. Synthesis and Characterization of Nearly Monodisperse CdE (E = Sulfur, Selenium, Tellurium) Semiconductor Nanocrystallites. *J. Am. Chem. Soc.* **1993**, *115* (19), 8706–8715.
- (2) Hanifi, D. A.; Bronstein, N. D.; Koscher, B. A.; Nett, Z.; Swabeck, J. K.; Takano, K.; Schwartzberg, A. M.; Maserati, L.; Vandewal, K.; van de Burgt, Y.; Salleo, A.; Alivisatos, A. P. Redefining Near-Unity Luminescence in Quantum Dots with Photothermal Threshold Quantum Yield. *Science* **2019**, *363* (6432), 1199–1202.
- (3) Murray, C. B.; Kagan, C. R.; Bawendi, M. G. Synthesis and Characterization of Monodisperse Nanocrystals and Close-Packed Nanocrystal Assemblies. *Annu. Rev. Mater. Sci.* **2000**, 30 (1), 545–610.
- (4) Kagan, C. R.; Lifshitz, E.; Sargent, E. H.; Talapin, D. V. Building Devices from Colloidal Quantum Dots. *Science* **2016**, 353 (6302), aac 5523
- (5) Whitworth, G. L.; Dalmases, M.; Taghipour, N.; Konstantatos, G. Solution-Processed PbS Quantum Dot Infrared Laser with Room-Temperature *T*unable Emission in the Optical Telecommunications Window. *Nat. Photonics* **2021**, *15* (10), 738–742.
- (6) Geiregat, P.; Van Thourhout, D.; Hens, Z. A Bright Future for Colloidal Quantum Dot Lasers. NPG Asia Mater. 2019, 11 (1), 1-8.
- (7) Park, Y.-S.; Roh, J.; Diroll, B. T.; Schaller, R. D.; Klimov, V. I. Colloidal Quantum Dot Lasers. *Nat. Rev. Mater.* **2021**, *6* (5), 382–401
- (8) Asada, M.; Miyamoto, Y.; Suematsu, Y. Gain and the Threshold of Three-Dimensional Quantum-Box Lasers. *IEEE J. Quantum Electron.* **1986**, 22 (9), 1915–1921.
- (9) Vandyshev, Yu. V.; Dneprovskii, V. S.; Klimov, V. I.; Okorokov, D. K. Lasing on a Transition between Quantum-Well Levels in a Quantum Dot. *ZhETF Pisma Redaktsiiu* 1991, 54, 441.
- (10) Klimov, V. I.; Mikhailovsky, A. A.; Xu, S.; Malko, A.; Hollingsworth, J. A.; Leatherdale, C. A.; Eisler, H.-J.; Bawendi, M. G. Optical Gain and Stimulated Emission in Nanocrystal Quantum Dots. *Science* **2000**, *290* (5490), 314–317.
- (11) Chen, Y.; Vela, J.; Htoon, H.; Casson, J. L.; Werder, D. J.; Bussian, D. A.; Klimov, V. I.; Hollingsworth, J. A. Giant" Multishell CdSe Nanocrystal Quantum Dots with Suppressed Blinking. *J. Am. Chem. Soc.* 2008, 130 (15), 5026–5027.
- (12) Vela, J.; Htoon, H.; Chen, Y.; Park, Y.-S.; Ghosh, Y.; Goodwin, P. M.; Werner, J. H.; Wells, N. P.; Casson, J. L.; Hollingsworth, J. A. Effect of Shell Thickness and Composition on Blinking Suppression and the Blinking Mechanism in 'Giant' CdSe/CdS Nanocrystal Quantum Dots. J. Biophotonics 2010, 3 (10–11), 706–717.
- (13) García-Santamaría, F.; Chen, Y.; Vela, J.; Schaller, R. D.; Hollingsworth, J. A.; Klimov, V. I. Suppressed Auger Recombination in "Giant" Nanocrystals Boosts Optical Gain Performance. *Nano Lett.* **2009**, *9* (10), 3482–3488.
- (14) Lim, J.; Park, Y.-S.; Klimov, V. I. Optical Gain in Colloidal Quantum Dots Achieved with Direct-Current Electrical Pumping. *Nat. Mater.* **2018**, *17*, 42–49.
- (15) Walsh, B. R.; Saari, J. I.; Krause, M. M.; Mack, T. G.; Nick, R.; Coe-Sullivan, S.; Kambhampati, P. Interfacial Electronic Structure in Graded Shell Nanocrystals Dictates Their Performance for Optical Gain. J. Phys. Chem. C 2016, 120 (34), 19409–19415.

- (16) Jung, H.; Park, Y.-S.; Ahn, N.; Lim, J.; Fedin, I.; Livache, C.; Klimov, V. I. Two-Band Optical Gain and Ultrabright Electroluminescence from Colloidal Quantum Dots at 1000 A Cm-2. *Nat. Commun.* **2022**, *13* (1), 3734.
- (17) Wintzheimer, S.; Granath, T.; Oppmann, M.; Kister, T.; Thai, T.; Kraus, T.; Vogel, N.; Mandel, K. Supraparticles: Functionality from Uniform Structural Motifs. *ACS Nano* **2018**, *12* (6), 5093–5120.
- (18) Zhang, M.; Magagnosc, D. J.; Liberal, I.; Yu, Y.; Yun, H.; Yang, H.; Wu, Y.; Guo, J.; Chen, W.; Shin, Y. J.; Stein, A.; Kikkawa, J. M.; Engheta, N.; Gianola, D. S.; Murray, C. B.; Kagan, C. R. High-Strength Magnetically Switchable Plasmonic Nanorods Assembled from a Binary Nanocrystal Mixture. *Nat. Nanotechnol.* **2017**, *12* (3), 228–232.
- (19) Zhang, M.; Guo, J.; Yu, Y.; Wu, Y.; Yun, H.; Jishkariani, D.; Chen, W.; Greybush, N. J.; Kübel, C.; Stein, A.; Murray, C. B.; Kagan, C. R. 3D Nanofabrication via Chemo-Mechanical Transformation of Nanocrystal/Bulk Heterostructures. *Adv. Mater.* **2018**, *30* (22), 1800233
- (20) Montanarella, F.; Altantzis, T.; Zanaga, D.; Rabouw, F. T.; Bals, S.; Baesjou, P.; Vanmaekelbergh, D.; van Blaaderen, A. Composite Supraparticles with Tunable Light Emission. *ACS Nano* **2017**, *11* (9), 9136–9142.
- (21) Vanmaekelbergh, D.; van Vugt, L. K.; Bakker, H. E.; Rabouw, F. T.; de Nijs, B.; van Dijk-Moes, R. J. A.; van Huis, M. A.; Baesjou, P. J.; van Blaaderen, A. Shape-Dependent Multiexciton Emission and Whispering Gallery Modes in Supraparticles of CdSe/Multishell Quantum Dots. ACS Nano 2015, 9 (4), 3942–3950.
- (22) Marino, E.; Bharti, H.; Xu, J.; Kagan, C. R.; Murray, C. B. Nanocrystal Superparticles with Whispering-Gallery Modes Tunable through Chemical and Optical Triggers. *Nano Lett.* **2022**, 22 (12), 4765–4773.
- (23) Montanarella, F.; Urbonas, D.; Chadwick, L.; Moerman, P. G.; Baesjou, P. J.; Mahrt, R. F.; van Blaaderen, A.; Stöferle, T.; Vanmaekelbergh, D. Lasing Supraparticles Self-Assembled from Nanocrystals. *ACS Nano* **2018**, *12* (12), 12788–12794.
- (24) Marino, E.; van Dongen, S. W.; Neuhaus, S. J.; Li, W.; Keller, A. W.; Kagan, C. R.; Kodger, T. E.; Murray, C. B. Monodisperse Nanocrystal Superparticles through a Source—Sink Emulsion System. *Chem. Mater.* **2022**, 34 (6), 2779–2789.
- (25) le Feber, B.; Prins, F.; De Leo, E.; Rabouw, F. T.; Norris, D. J. Colloidal-Quantum-Dot Ring Lasers with Active Color Control. *Nano Lett.* **2018**, *18* (2), 1028–1034.
- (26) Galland, C.; Ghosh, Y.; Steinbrück, A.; Sykora, M.; Hollingsworth, J. A.; Klimov, V. I.; Htoon, H. Two Types of Luminescence Blinking Revealed by Spectroelectrochemistry of Single Quantum Dots. *Nature* **2011**, *479* (7372), 203–207.
- (27) Marino, E.; Kodger, T. E.; Wegdam, G. H.; Schall, P. Revealing Driving Forces in Quantum Dot Supercrystal Assembly. *Adv. Mater.* **2018**, *30* (43), 1803433.
- (28) Savo, R.; Morandi, A.; Müller, J. S.; Kaufmann, F.; Timpu, F.; Reig Escalé, M.; Zanini, M.; Isa, L.; Grange, R. Broadband Mie Driven Random Quasi-Phase-Matching. *Nat. Photonics* **2020**, *14* (12), 740–747
- (29) Oraevsky, A. N. Whispering-Gallery Waves. *Quantum Electron* **2002**, 32 (5), 377–400.
- (30) Reynolds, T.; Riesen, N.; Meldrum, A.; Fan, X.; Hall, J. M. M.; Monro, T. M.; François, A. Fluorescent and Lasing Whispering Gallery Mode Microresonators for Sensing Applications. *Laser Photonics Rev.* **2017**, *11* (2), 1600265.
- (31) Foreman, M. R.; Swaim, J. D.; Vollmer, F. Whispering Gallery Mode Sensors. *Adv. Opt. Photonics* **2015**, *7* (2), 168.
- (32) Bisschop, S.; Geiregat, P.; Aubert, T.; Hens, Z. The Impact of Core/Shell Sizes on the Optical Gain Characteristics of CdSe/CdS Quantum Dots. ACS Nano 2018, 12 (9), 9011–9021.
- (33) Cihan, A. F.; Kelestemur, Y.; Guzelturk, B.; Yerli, O.; Kurum, U.; Yaglioglu, H. G.; Elmali, A.; Demir, H. V. Attractive versus Repulsive Excitonic Interactions of Colloidal Quantum Dots Control

Nano Letters pubs.acs.org/NanoLett Letter

Blue- to Red-Shifting (and Non-Shifting) Amplified Spontaneous Emission. J. Phys. Chem. Lett. 2013, 4 (23), 4146-4152.

- (34) Newville, M.; Stensitzki, T.; Allen, D. B.; Ingargiola, A.LMFIT: Non-Linear Least-Square Minimization and Curve-Fitting for Python,
- (35) Vollmer, F.; Yu, D.Optical Whispering Gallery Modes for Biosensing: From Physical Principles to Applications; Biological and Medical Physics, Biomedical Engineering; Springer International Publishing: Cham, 2020.
- (36) Orfield, N. J.; Majumder, S.; McBride, J. R.; Yik-Ching Koh, F.; Singh, A.; Bouquin, S. J.; Casson, J. L.; Johnson, A. D.; Sun, L.; Li, X.; Shih, C.-K.; Rosenthal, S. J.; Hollingsworth, J. A.; Htoon, H. Photophysics of Thermally-Assisted Photobleaching in "Giant" Quantum Dots Revealed in Single Nanocrystals. ACS Nano 2018, 12 (5), 4206-4217.
- (37) Schubert, M.; Woolfson, L.; Barnard, I. R. M.; Dorward, A. M.; Casement, B.; Morton, A.; Robertson, G. B.; Appleton, P. L.; Miles, G. B.; Tucker, C. S.; Pitt, S. J.; Gather, M. C. Monitoring Contractility in Cardiac Tissue with Cellular Resolution Using Biointegrated Microlasers. Nat. Photonics 2020, 14 (7), 452-458.
- (38) Beane, G. A.; Gong, K.; Kelley, D. F. Auger and Carrier Trapping Dynamics in Core/Shell Quantum Dots Having Sharp and Alloyed Interfaces. ACS Nano 2016, 10 (3), 3755-3765.
- (39) Klimov, V. I. Multicarrier Interactions in Semiconductor Nanocrystals in Relation to the Phenomena of Auger Recombination and Carrier Multiplication. Annu. Rev. Condens. Matter Phys. 2014, 5 (1), 285-316.
- (40) Wu, K.; Lim, J.; Klimov, V. I. Superposition Principle in Auger Recombination of Charged and Neutral Multicarrier States in Semiconductor Quantum Dots. ACS Nano 2017, 11 (8), 8437-8447.

□ Recommended by ACS

Ultrafast Control of the Optical Transition in Type-II **Colloidal Quantum Wells**

Junhong Yu, Cuong Dang, et al.

APRIL 21, 2023 ACS PHOTONICS

READ 2

Excitation Intensity-Dependent Quantum Yield of Semiconductor Nanocrystals

Subhabrata Ghosh, Alexev I. Chizhik, et al.

MARCH 09, 2023

THE JOURNAL OF PHYSICAL CHEMISTRY LETTERS

READ **C**

FRET-Mediated Collective Blinking of Self-Assembled Stacks of CdSe Semiconducting Nanoplatelets

Zakarya Ouzit, Laurent Coolen, et al.

JANUARY 26, 2023

ACS PHOTONICS

READ **C**

Visible and Infrared Nanocrystal-Based Light Modulator with CMOS Compatible Bias Operation

Huichen Zhang, Emmanuel Lhuillier, et al.

JANUARY 26, 2023

ACS PHOTONICS

READ 2

Get More Suggestions >